

ARTICLE



The membrane-associated ubiquitin ligases MARCH2 and MARCH3 target IL-5 receptor alpha to negatively regulate eosinophilic airway inflammation

Lin-Wen Zeng¹, Lu Feng¹, Rui Liu¹, Heng Lin¹, Hong-Bing Shu¹ and Shu Li¹ ✉

© The Author(s), under exclusive licence to CSI and USTC 2022

Interleukin 5 (IL-5) plays crucial roles in type 2-high asthma by mediating eosinophil maturation, activation, chemotaxis and survival. Inhibition of IL-5 signaling is considered a strategy for asthma treatment. Here, we identified MARCH2 and MARCH3 as critical negative regulators of IL-5-triggered signaling. MARCH2 and MARCH3 associate with the IL-5 receptor α chain (IL-5R α) and mediate its K27-linked polyubiquitination at K379 and K383, respectively, and its subsequent lysosomal degradation. Deficiency of MARCH2 or MARCH3 modestly increases the level of IL-5R α and enhances IL-5-induced signaling, whereas double knockout of MARCH2/3 has a more dramatic effect. MARCH2/3 double knockout markedly increases the proportions of eosinophils in the bone marrow and peripheral blood in mice. Double knockout of MARCH2/3 aggravates ovalbumin (OVA)-induced eosinophilia and causes increased inflammatory cell infiltration, peribronchial mucus secretion and production of Th2 cytokines. Neutralization of IL-5 attenuates OVA-induced airway inflammation and the enhanced effects of MARCH2/3 double deficiency. These findings suggest that MARCH2 and MARCH3 play redundant roles in targeting IL-5R α for degradation and negatively regulating allergic airway inflammation.

Keywords: MARCH2/3; IL-5R α ; Polyubiquitination; Eosinophil; Airway inflammation

Cellular & Molecular Immunology (2022) 19:1117–1129; <https://doi.org/10.1038/s41423-022-00907-9>

INTRODUCTION

IL-5 is recognized as the major factor for eosinophil maturation and differentiation in mice and humans [1, 2]. Eosinophil progenitors mature in the bone marrow and acquire IL-5 receptor expression before being released into the peripheral blood. Eosinophils either stay in the bone marrow or enter various peripheral tissues, where they exert homeostatic functions, including maintenance of plasma cells and metabolic homeostasis [3, 4]. Direct targeting of the eosinophil differentiation process has been considered an effective therapeutic strategy to treat clinical symptoms of asthma and reduce exacerbations [5–8]. In type 2-high asthma, eosinophils are recruited from the bloodstream to the lung, where they are activated by IL-5 released by Th2 cells. Intraperitoneal injection of anti-IL-5 inhibits both bone marrow and airway eosinophilia. Intranasal administration of anti-IL-5 also reduces bronchoalveolar lavage fluid (BALF) eosinophilia, partially due to local effects in the airways. Bone marrow cells but not BALF eosinophils contain stainable amounts of IL-5 receptor alpha chain (IL-5R α), suggesting that bone marrow IL-5 and IL-5R α are involved in eosinophilopoiesis in allergic airway eosinophilia [9].

IL-5 binds to a heterodimeric receptor complex comprising IL-5-specific IL-5R α and the β chain receptor (IL-5R β), which is also shared by the β common chain family members IL-3 and granulocyte-macrophage colony-stimulating factor (GM-CSF) [2, 10]. Binding of

IL-5 to its receptor complex induces rapid tyrosine phosphorylation of Janus kinases (JAKs) [11, 12]. The activated JAKs then recruit the transcription factor signal transducer and activator of transcription 5 (STAT5) and mediate its phosphorylation [13]. Phosphorylation of STAT5 leads to its translocation into the nucleus to induce the transcription of downstream effector genes, such as *PIM-1*, *ID1* and *CD69*, which are essential for the survival, proliferation and differentiation of eosinophils [14, 15]. Studies on *Stat5a*^{-/-} mice and *Stat5b*^{-/-} mice have shown that defects in antigen-induced eosinophil recruitment arise from both impaired IL-5 production in the airways and the diminished IL-5 responsiveness of eosinophils [16]. The Th2 cytokine IL-5 but not IL-13 or IL-25 is able to induce the development of IL-4-producing eosinophils independent of IL-4. The ability of IL-5 to drive bone marrow progenitors to differentiate primarily into IL-4-producing eosinophils is completely dependent on Stat5 α/β [17]. These studies highlight the important roles of IL-5 signaling in the regulation of Th2- and eosinophil-associated inflammation. Most previous studies on the regulation of IL-5 signaling have focused on its downstream signaling events, and where and how it is regulated at the receptor level are largely unknown.

The membrane-associated RING-CH-type finger (MARCH) proteins are a subfamily of E3 ubiquitin ligases. Unlike MARCH7 and MARCH10, the other 9 members of the family contain at least one transmembrane domain and are located at the plasma membrane

¹Department of Infectious Diseases, Zhongnan Hospital of Wuhan University; Medical Research Institute; Frontier Science Center for Immunology and Metabolism; Research Unit of Innate Immune and Inflammatory Diseases (2019RU063), Chinese Academy of Medical Sciences; Wuhan University, Wuhan 430071, China. ✉email: shuli@whu.edu.cn

Received: 9 February 2022 Accepted: 12 July 2022

Published online: 19 August 2022

or organelle membranes [18]. Recent studies suggest that MARCH family proteins are mediate the regulation of immune responses by targeting certain immune receptors, organelle membrane-associated components and signaling components [19, 20]. For example, it has been shown that MARCH3 and MARCH8 target IL-1 receptor I (IL-1RI) and IL-1 receptor associated protein (IL-1RAP), respectively, for polyubiquitination and degradation to negatively regulate the IL-1-triggered inflammatory response [21, 22]. MARCH3 also targets the IL-6 receptor and suppresses colitis-associated carcinogenesis [23]. In this study, we found that two closely related MARCH family members, MARCH2 and MARCH3, target IL-5R α for its K27-linked polyubiquitination and lysosomal degradation, thereby negatively regulating IL-5-triggered signaling in a redundant manner. Double knockout of MARCH2/3 in mice markedly increases the percentages of eosinophils in the bone marrow and peripheral blood and aggravates ovalbumin (OVA)-induced systemic eosinophilia and asthmatic responses. Our findings reveal a redundant role of MARCH2 and MARCH3 in targeting IL-5R α for degradation and negatively regulating allergic airway inflammation.

RESULTS

MARCH2/3 negatively regulate IL-5-triggered signaling by downregulating IL-5R α

We previously demonstrated that MARCH3 and MARCH8 can target the IL-1 and IL-6 receptors, respectively [21–23]. In this study, we investigated the potential regulatory roles of MARCH proteins in IL-5-triggered signaling. We cotransfected each of the 11 MARCH family proteins with IL-5R α and examined their regulation of the IL-5R α level. This screen indicated that overexpression of MARCH2 or MARCH3 but not the other MARCH proteins caused a decrease in the IL-5R α level (Fig. 1A). Overexpression of MARCH2 or MARCH3 mediated the degradation of IL-5R α but not IL-5R β in a dose-dependent manner (Fig. 1B). To investigate the roles of endogenous MARCH2 and MARCH3, we generated MARCH2-, MARCH3- and MARCH2/3 double-deficient human hemopoietic TF-1-IL5 cells (which are IL-5 dependent) by CRISPR/Cas9 [24, 25]. Immunoblot (IB) analysis indicated that the level of endogenous IL-5R α was modestly increased in cells deficient in either MARCH2 or MARCH3 and more markedly increased in MARCH2/3 double-deficient cells (Fig. 1C). In the same experiments, MARCH2 or MARCH3 deficiency had no marked effects on the IL-5R β level (Fig. 1C). Consistent with this finding, immunoblot analysis indicated that MARCH2 or MARCH3 deficiency modestly increased IL-5-induced phosphorylation of STAT5 at Y694/699 (which is a hallmark of its activation), whereas double knockout of MARCH2/3 caused more dramatic increases in IL-5-induced STAT5^{Y694/699} phosphorylation in TF-1-IL5 cells (Fig. 1D). In addition, MARCH2 or MARCH3 deficiency modestly increased the IL-5-induced transcription of the downstream genes *CD69*, *PIM1* and *ID1* in TF-1-IL5 cells, whereas double knockout of MARCH2/3 had more dramatic effects (Fig. 1E). In similar experiments, the transcription of the downstream genes *CD69*, *PIM1* and *ID1* induced by GM-CSF was comparable between control and MARCH2-deficient, MARCH3-deficient or MARCH2/3 double-deficient cells (Fig. 1E). We reconstituted MARCH2/3-deficient TF-1-IL5 cells with MARCH2, MARCH3 or both MARCH2 and 3. qPCR experiments indicated that reconstitution of MARCH2 or MARCH3 attenuated the increases in the mRNA transcription of *CD69* and *PIM1* triggered by IL-5 in MARCH2/3-deficient TF-1-IL5 cells and that reconstitution of both MARCH2 and 3 had a more pronounced effect (Fig. S1). These data suggest that endogenous MARCH2/3 negatively regulate IL-5-triggered signaling in TF-1-IL5 cells through regulation of the IL-5R α level.

MARCH2/3 mediates K27-linked polyubiquitination and lysosomal degradation of IL-5R α

To investigate the molecular mechanisms responsible for the inhibitory effects of MARCH2/3 on IL-5-triggered signaling, we

examined whether MARCH2 and MARCH3 are associated with components in IL5-triggered signaling pathways. Mammalian overexpression and coimmunoprecipitation (co-IP) experiments indicated that MARCH2 and MARCH3 were strongly associated with IL-5R α and weakly associated with IL-5R β but were not associated with the other examined downstream components, including JAK1, JAK2, STAT5A and STAT5B (Fig. 2A). Endogenous coimmunoprecipitation experiments showed that MARCH2 and MARCH3 were constitutively associated with IL-5R α (Fig. 2B). After IL-5 stimulation, the association between MARCH2 and IL-5R α was slightly enhanced, while the association between MARCH3 and IL-5R α was slightly decreased (Fig. 2B).

Since MARCH proteins are RING-type E3 ubiquitin ligases, we next investigated whether MARCH2 and MARCH3 mediate the polyubiquitination of IL-5R α . In the mammalian overexpression system, wild-type (WT) MARCH2 or MARCH3 but not their ligase-inactive mutants (MARCH2 C67S, C67S, and C80S; MARCH3 C71S, C74S, and C87S) promoted the polyubiquitination and degradation of IL-5R α (Fig. 2C). We next determined the types of ubiquitin chains conjugated by MARCH2 and MARCH3. By cotransfection of IL-5R α with ubiquitin mutants containing only a single lysine residue (KO), we found that both MARCH2 and MARCH3 promoted K27-linked polyubiquitination of IL-5R α . By cotransfection of IL-5R α with ubiquitin mutants in which only one lysine residue was mutated to arginine, we found that MARCH2 and MARCH3 failed to promote the polyubiquitination of IL-5R α only when K27 was mutated to arginine (Fig. 2D). These results suggest that MARCH2/3 mediates K27-linked polyubiquitination of IL-5R α . Consistent with this finding, IL-5-induced K27-linked polyubiquitination of endogenous IL-5R α was inhibited in MARCH2/3 double-deficient TF-1-IL5 cells, in which the IL-5R α level was markedly higher than that in control cells (Fig. 2E). Taken together, our results suggest that MARCH2/3 mediates K27-linked polyubiquitination and degradation of IL-5R α .

To further explore the mechanisms responsible for polyubiquitination-primed degradation of IL-5R α , we treated HEK293 cells with inhibitors of various protein degradation pathways. Immunoblot analysis indicated that the downregulation of IL-5R α mediated by MARCH2 and MARCH3 was reversed by treatment of the cells with the lysosome inhibitor NH₄Cl but not the proteasome inhibitor MG132 or the autophagosome inhibitor 3-methyladenine (3-MA) (Fig. 2F). Consistent with this finding, NH₄Cl markedly inhibited IL-5R α degradation after termination of protein synthesis by cycloheximide (Fig. 2G). These results suggest that MARCH2/3-mediated K27-linked polyubiquitination of IL-5R α leads to its lysosomal degradation.

It has been demonstrated that MARCH-mediated polyubiquitination takes place on the cytosolic side of the plasma membrane, in line with the binding of E2 proteins to the cytosolic RING-CH domains of MARCH proteins [26, 27]. Sequence analysis indicated that six lysine residues exist in the cytoplasmic domain (aa 363–420) of human IL-5R α (Fig. 3A). To identify the potential polyubiquitination sites, we individually mutated each of these lysine residues in IL-5R α to arginine and examined whether these mutants could be modified by MARCH2 or MARCH3. The results indicate that mutation of K379 but not the other lysine residues abolished MARCH2-mediated K27-linked polyubiquitination, whereas mutation of K383 but not the other lysine residues abolished MARCH3-mediated K27-linked polyubiquitination (Fig. 3B). Consistent with this finding, the MARCH2-mediated downregulation of IL-5R α ^{K379R} and MARCH3-mediated downregulation of IL-5R α ^{K383R} were impaired (Fig. 3C). Sequence analysis showed that K379 and K383 but not the other lysine residues in human IL-5R α are conserved across species (Fig. 3A), consistent with the conserved roles of these two lysine residues in the regulation of IL-5R α by MARCH2/3.

Confocal microscopy showed that IL-5R α was colocalized with MARCH2/3 on the plasma membrane and lysosomal membrane (Fig. 3D). However, IL-5R α ^{K379R} and IL-5R α ^{K383R} failed to be

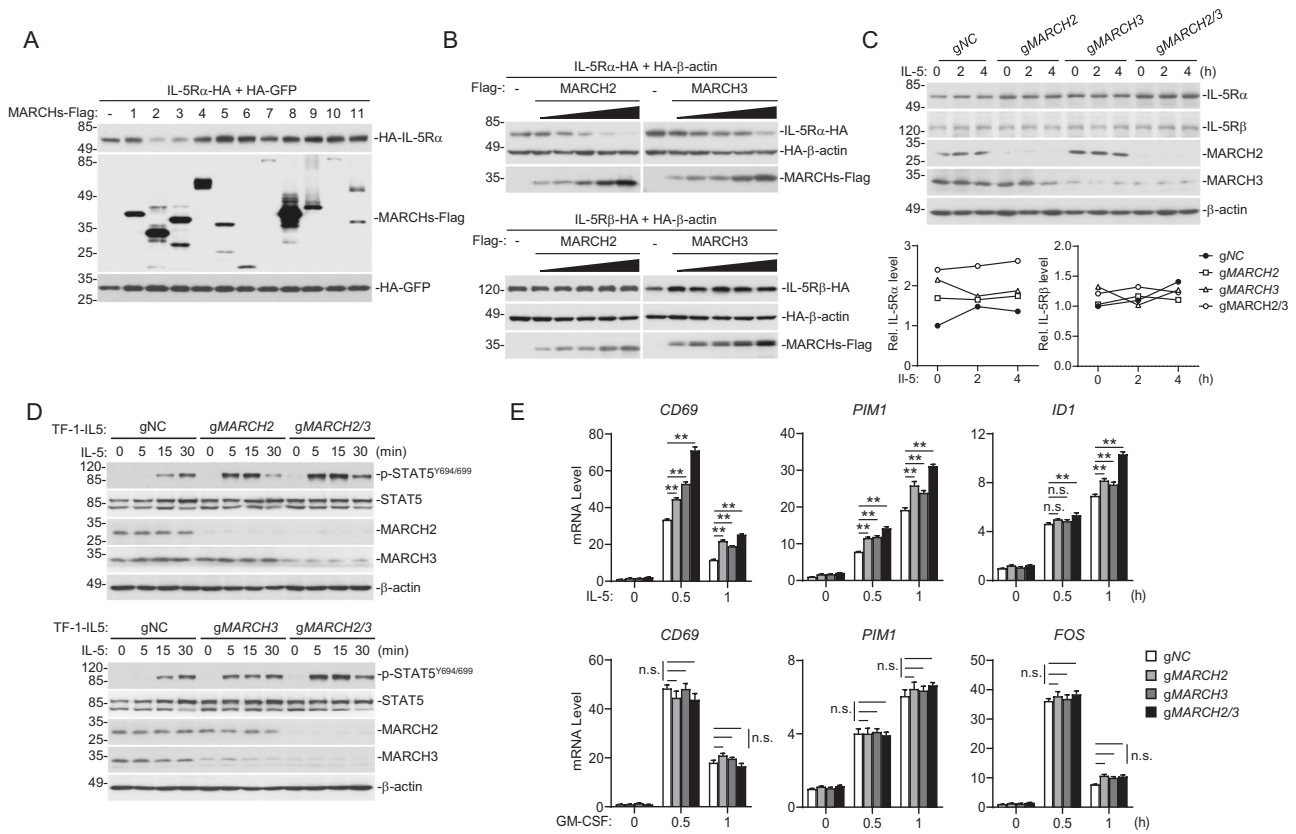


Fig. 1 MARCH2/3 negatively regulates IL-5-triggered signaling by downregulating IL-5R α . **A** Effects of MARCH protein overexpression on the IL-5R α protein level. HEK293 cells were transfected with the indicated plasmids for 24 h before immunoblot analysis with the indicated antibodies. **B** MARCH2 and MARCH3 promote the degradation of IL-5R α but not IL-5R β in a dose-dependent manner. HEK293 cells were transfected with the indicated plasmids for 24 h before immunoblot analysis with the indicated antibodies. **C** Effects of MARCH2, MARCH3 and MARCH2/3 deficiency on the IL-5R α protein level. TF-1-IL5 cells were starved overnight by removal of recombinant IL-5 from the medium and were then stimulated with IL-5 (100 ng/mL) for the indicated times before immunoblot analysis with the indicated antibodies. The lower graph shows the levels of IL-5R α and IL-5R β relative to β -actin, as quantified by ImageJ. **D** Effects of MARCH2, MARCH3 and MARCH2/3 deficiency on IL-5-induced phosphorylation of STAT5^{Y694/699} in TF-1-IL5 cells. KO and control TF-1-IL5 cells were starved overnight by removal of recombinant IL-5 from the medium and were then left untreated or treated with IL-5 (100 ng/mL) for the indicated times before immunoblot analysis. **E** Effects of MARCH2, MARCH3 and MARCH2/3 deficiency on the transcription of downstream genes induced by IL-5 and GM-CSF in TF-1-IL5 cells. KO and control TF-1-IL5 cells were starved overnight and then left untreated or treated with IL-5 (20 ng/mL) or GM-CSF (20 ng/mL) for the indicated times before qPCR analysis. The data shown are the means \pm SEMs; $n = 3$ technical replicates. ** $P < 0.01$; n.s. not significant. IB immunoblot. All experiments were repeated at least two times with similar results

internalized into lysosomes (Fig. 3D). These results further confirm that MARCH2/3-mediated K27-linked polyubiquitination of IL-5R α at K379 and K383 causes its translocation to lysosomes for degradation. Consistent with this finding, reconstitution of IL-5R α ^{K379/383R} in IL-5R α -deficient cells increased IL-5-induced transcription of the downstream genes *CD69*, *ID1* and *PIM1* in comparison to cells reconstituted with wild-type IL-5R α (Fig. 3E). Taken together, these results suggest that MARCH2 and MARCH3 mediate K27-linked polyubiquitination of IL-5R α at K379 and K383, respectively, resulting in its translocation to and degradation in lysosomes.

March2/3 negatively regulates eosinophil maturation

To further investigate the roles of March proteins in vivo, we generated March2- and March3-deficient mice by CRISPR/Cas9 [23] and obtained March2/3 double-deficient mice by breeding. Deficiency of March2 and March3 was confirmed by immunoblot analysis of splenocytes (Fig. S2A).

Common myeloid progenitors (CMPs) differentiated from hematopoietic stem cells (HSCs) give rise to granulocyte-macrophage progenitors (GMPs) [28]. The eosinophil developmental pathway diverges from that of neutrophils and monocytes at the GMP stage, which results in the development of eosinophil

progenitors (EoPs) [29]. EoPs acquire IL-5 receptor expression and mature into eosinophils (Eos), which are released into the peripheral blood [30] (Fig. 4A). It has been demonstrated that IL-5 is the major factor for eosinophil maturation and differentiation in mammals [2]. To investigate whether March2 and March3 regulate eosinophil maturation in vivo, we prepared wild-type, *March2*^{-/-}, *March3*^{-/-} and *March2*^{-/-}/*March3*^{-/-} bone marrow and peripheral blood cells and analyzed myeloid developmental subsets by flow cytometry. We first analyzed the *Il-5ra* level on the plasma membrane of eosinophils by flow cytometry. The results indicated that the median fluorescence intensity (MFI) of IL-5 α on *March2*^{-/-}/*March3*^{-/-} eosinophils was higher than that on wild-type eosinophils (Figs. 4B and S2B). Deficiency of only March2 or March3 caused a weaker or nonsignificant increase in the IL-5 α level on the plasma membrane (Figs. 4B and S2B), consistent with a redundant role of March2 and March3 in the regulation of the IL-5 α level. We also examined the level of intracellular IL-5 α by flow cytometry. The results showed that the median fluorescence intensity of intracellular IL-5 α in *March2*^{-/-}/*March3*^{-/-} eosinophils was markedly higher than that in wild-type eosinophils (Figs. 4B and S2B). To determine whether IL-5 signaling is regulated by March2 and March3 in eosinophils, we sorted CCR3⁺Siglec-F⁺ eosinophils from the bone marrow of wild-type and *March2*^{-/-}/*March3*^{-/-} mice.

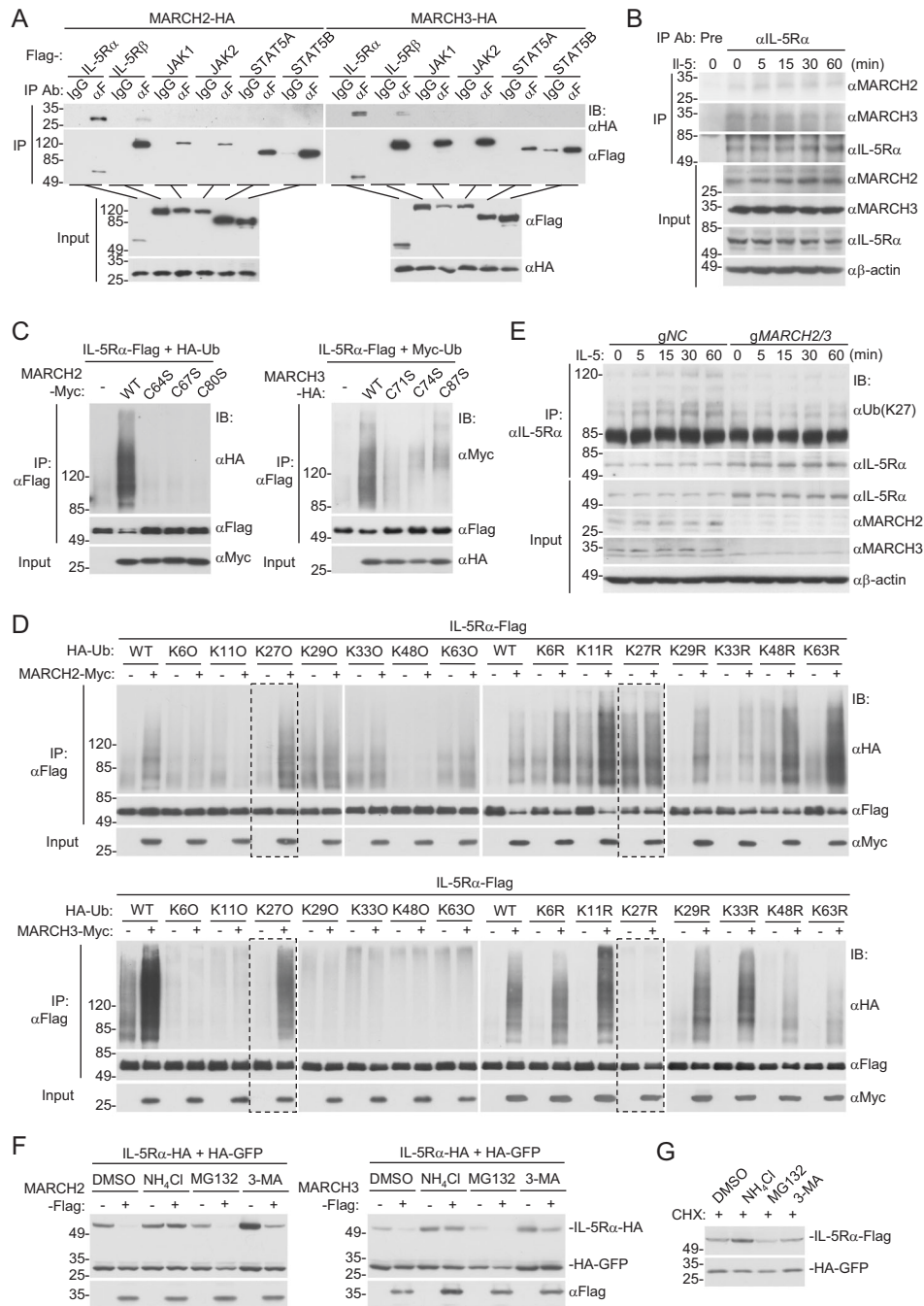


Fig. 2 MARCH2/3 mediates K27-linked polyubiquitination and lysosomal degradation of IL-5R α . **A** MARCH2 and MARCH3 interact strongly with IL-5R α and weakly with IL-5R β . HEK293 cells were transfected with the indicated plasmids for 20 h before coimmunoprecipitation (co-IP) and immunoblot analysis with the indicated antibodies. **B** Endogenous MARCH2 and MARCH3 associate with IL-5R α . TF-1-IL-5 cells were starved overnight by removal of recombinant IL-5 from the medium and were then left untreated or treated with IL-5 (100 ng/mL) for the indicated times before coimmunoprecipitation and immunoblot analysis with the indicated antibodies. **C** MARCH2 and not their E3 ligase-inactive mutants mediate the polyubiquitination of IL-5R α . HEK293 cells were transfected with the indicated plasmids for 24 h before coimmunoprecipitation and immunoblot analysis with the indicated antibodies. **D** MARCH2 and MARCH3 mediate K27-linked polyubiquitination of IL-5R α . HEK293 cells were transfected with the indicated plasmids for 18–20 h before coimmunoprecipitation and immunoblot analysis with the indicated antibodies. **E** Effects of MARCH2/3 deficiency on IL-5-induced K27-linked polyubiquitination of IL-5R α . Control and MARCH2/3-deficient TF-1-IL5 cells were starved overnight by removal of recombinant IL-5 from the medium and were then left untreated or treated with IL-5 (100 ng/mL) for the indicated times before coimmunoprecipitation and immunoblot analysis. KO, K only; KR, K mutated to R. **F** Effects of inhibitors on MARCH2- and MARCH3-mediated downregulation of IL-5R α . HEK293 cells were transfected with the indicated plasmids for 12 h and were then treated with NH₄Cl (25 mM), MG132 (100 μ M) or 3-MA (3.35 mM) for 6 h before immunoblot analysis with the indicated antibodies. **G** NH₄Cl inhibits IL-5R α degradation following CHX treatment. HEK293 cells were treated with CHX (0.1 mM) for 3 h and were then treated with NH₄Cl (25 mM), MG132 (100 μ M) or 3-MA (3.35 mM) for an additional 3 h before immunoblot analysis with the indicated antibodies. IB immunoblot, IP immunoprecipitation. All experiments were repeated at least two times with similar results

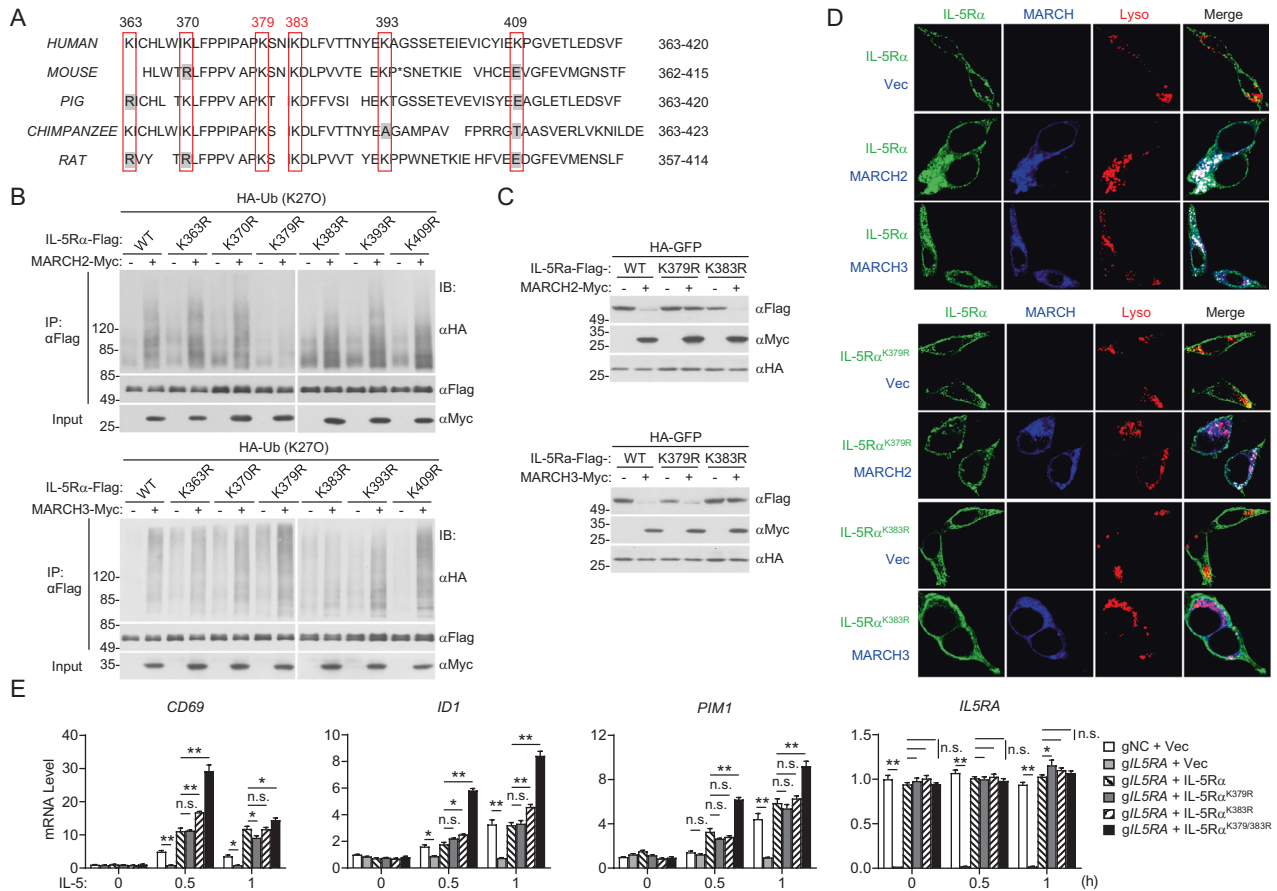


Fig. 3 MARCH2 and MARCH3 mediate the polyubiquitination of IL-5R α at K379 and K383, respectively. **A** Sequence alignment of the cytoplasmic domains of IL-5R α in the indicated species. The sequences correspond to aa 363-420 in human IL-5R α . **B** MARCH2 and MARCH3 mediate K27-linked polyubiquitination of IL-5R α at K379 and K383, respectively. HEK293 cells were transfected with the indicated plasmids for 18 h before coimmunoprecipitation and immunoblot analysis with the indicated antibodies. **C** Effects of MARCH2 and MARCH3 on the stability of IL-5R α and its mutants. HEK293 cells were transfected with the indicated plasmids for 24 h before immunoblot analysis with the indicated antibodies. **D** IL-5R α colocalizes with MARCH2 and MARCH3. HEK293 cells were transfected with FLAG-tagged IL-5R α , HA-tagged MARCH2 and HA-tagged MARCH3 for 20 h. The cells were stained with LysoTracker Red (200 nM) for 1 h and were then fixed with 4% paraformaldehyde and stained with mouse anti-FLAG and rabbit anti-HA antibodies. IL-5R α was labeled with an Alexa Fluor 488-conjugated secondary antibody, and MARCH2 and MARCH3 were labeled with an Alexa Fluor 647-conjugated secondary antibody. Images were acquired under a confocal microscope with a $\times 63$ oil objective. **E** Reconstitution of IL-5R α -deficient TF-1-IL5 cells with wild-type IL-5R α and its mutants. IL-5R α -deficient TF-1-IL5 cells were reconstituted with wild-type IL-5R α , IL-5R α ^{K379R}, IL-5R α ^{K383R}, IL-5R α ^{K379/383R} or empty vector by lentiviral-mediated transduction. The reconstituted cells were starved overnight by removal of recombinant IL-5 from the medium and were then stimulated with IL-5 (20 ng/ml) for the indicated times before qPCR analysis of the mRNA levels of the indicated genes. The data shown are the means \pm SEMs; $n = 3$ technical replicates. * $P < 0.05$; ** $P < 0.01$; n.s. not significant. IB immunoblot, IP immunoprecipitation. All experiments were repeated at least twice with similar results

The qPCR results indicated that March2 and March3 double deficiency in eosinophils enhanced the transcription of the downstream genes *Id1*, *Cish* and *Socs3* following IL-5 stimulation (Fig. S2C). Flow cytometric analysis also indicated that *March2*^{-/-}/*3*^{-/-} mice exhibited significantly larger populations of eosinophils in the bone marrow (Fig. 4C) and peripheral blood (Fig. 4D), whereas *March2*^{-/-} and *March3*^{-/-} mice had no marked or only modest increases in these eosinophil populations in comparison to those in wild-type mice (Fig. 4C, D). In these experiments, the CMP, GMP and EoP populations were comparable between March2/3-deficient and wild-type mice (Fig. 4E). Since IL-5 α expression is restricted to eosinophils and a subtype of B cells called B1 cells, we further determined the proportion of B1 cells and measured the expression of IL-5 α on B1 cells from the peritoneal and pleural cavities. The protein level of IL-5 α on B1 cells in *March2*^{-/-}/*3*^{-/-} mice was higher than that in wild-type mice, while the proportion of B1 cells showed no significant difference between wild-type and *March2*^{-/-}/*3*^{-/-} mice, suggesting that March2 and March3 negatively regulate the expression of

IL-5 α in vivo but do not regulate B1-cell proliferation (Fig. S2D, E). We also examined the effects of March2/3 deficiency on the development of T and B lymphocytes. These compositions of these cells in the peripheral blood and spleen were comparable between wild-type and March-deficient mice (Fig. 4F). These findings suggest that March2 and March3 negatively regulate IL-5 α expression in vivo and play redundant roles in the negative regulation of eosinophil maturation.

March2/3 deficiency promotes eosinophilic airway inflammation by enhancing IL-5 signaling

Previous studies have demonstrated a crucial role of IL-5 in eosinophilic inflammation in asthma [31]. The ovalbumin (OVA)-induced model of allergic asthma has been widely used for studying eosinophilic airway inflammation (Fig. 5A). Allergens can stimulate epithelial cells, leading to the production of cytokines such as IL-33. Epithelial cytokines subsequently stimulate DCs to promote naive CD4⁺ T-cell polarization to produce Th2 cytokines, including IL-5, leading to the maturation and activation of

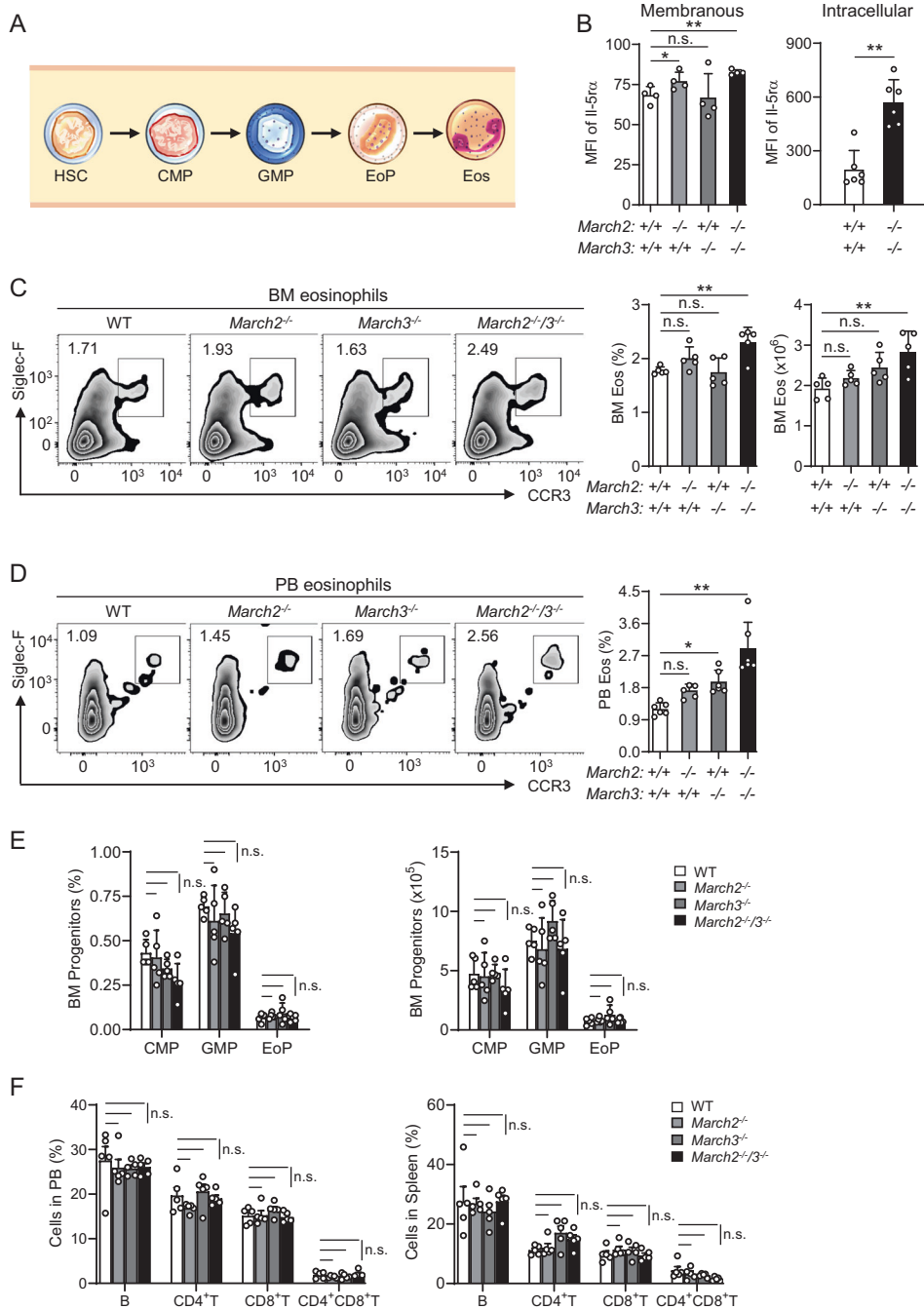


Fig. 4 March2/3 negatively regulate eosinophil maturation. **A** A model for eosinophil development in mouse bone marrow. HSC, hematopoietic stem cell; CMP, common myeloid progenitor; GMP, granulocyte-macrophage progenitor; EoP, eosinophil progenitor; Eos, eosinophil. **B** Effects of March deficiency on the levels of plasma membrane (left) and intracellular (right) Il-5 α in bone marrow CCR3⁺Siglec-F⁺ eosinophils. Bone marrow cells from sex- and age-matched wild-type, *March2*^{-/-}, *March3*^{-/-} and *March2*^{-/-}/*3*^{-/-} mice were stained with the indicated antibodies and analyzed by flow cytometry. The data shown are the means \pm SDs; $n = 4$ mice per group (left) and $n = 6$ mice per group (right), both from one representative experiment. MFI, median fluorescence intensity. Effects of March deficiency on the numbers and percentages of CCR3⁺Siglec-F⁺ eosinophils in the bone marrow (**C**) and peripheral blood (**D**). The left panels show representative flow cytometric plots, and the histograms on the right show analyses of cell numbers or percentages. Bone marrow and peripheral blood leukocytes from sex- and age-matched wild-type, *March2*^{-/-}, *March3*^{-/-} and *March2*^{-/-}/*3*^{-/-} mice were stained with the indicated antibodies and analyzed by flow cytometry. The data shown are the means \pm SDs; $n = 5$ mice per group (**C**) or $n = 6$ mice per group (**D**). Data from two independent experiments were combined. **E** Effects of March deficiency on the percentages and numbers of progenitors in the bone marrow. Bone marrow cells from sex- and age-matched wild-type, *March2*^{-/-}, *March3*^{-/-} and *March2*^{-/-}/*3*^{-/-} mice were analyzed for the percentages and numbers of Lin⁻c-Kit⁺CD34⁺CD16/32^{int} CMPs, Lin⁻c-Kit⁺CD34⁺CD16/32⁺ GMPs and Lin⁻CD34⁺Sca1⁻c-Kit^{int}Il-5 α ⁺ EoPs. The data shown are the means \pm SDs; $n = 5$ mice per group. Data from two independent experiments were combined. **F** Effects of March deficiency on the percentages of B and T cells in the peripheral blood (left) and spleen (right). Peripheral blood leukocytes and splenocytes from sex- and age-matched wild-type, *March2*^{-/-}, *March3*^{-/-} and *March2*^{-/-}/*3*^{-/-} mice were stained to identify B220⁺ B cells, CD3⁺CD4⁺ T cells, CD3⁺CD8⁺ T cells and CD3⁺CD4⁺CD8⁺ T cells and analyzed by flow cytometry. The data shown are the means \pm SDs; $n = 5$ mice per group from one representative experiment. WT wild-type. * $P < 0.05$; ** $P < 0.01$; n.s. not significant

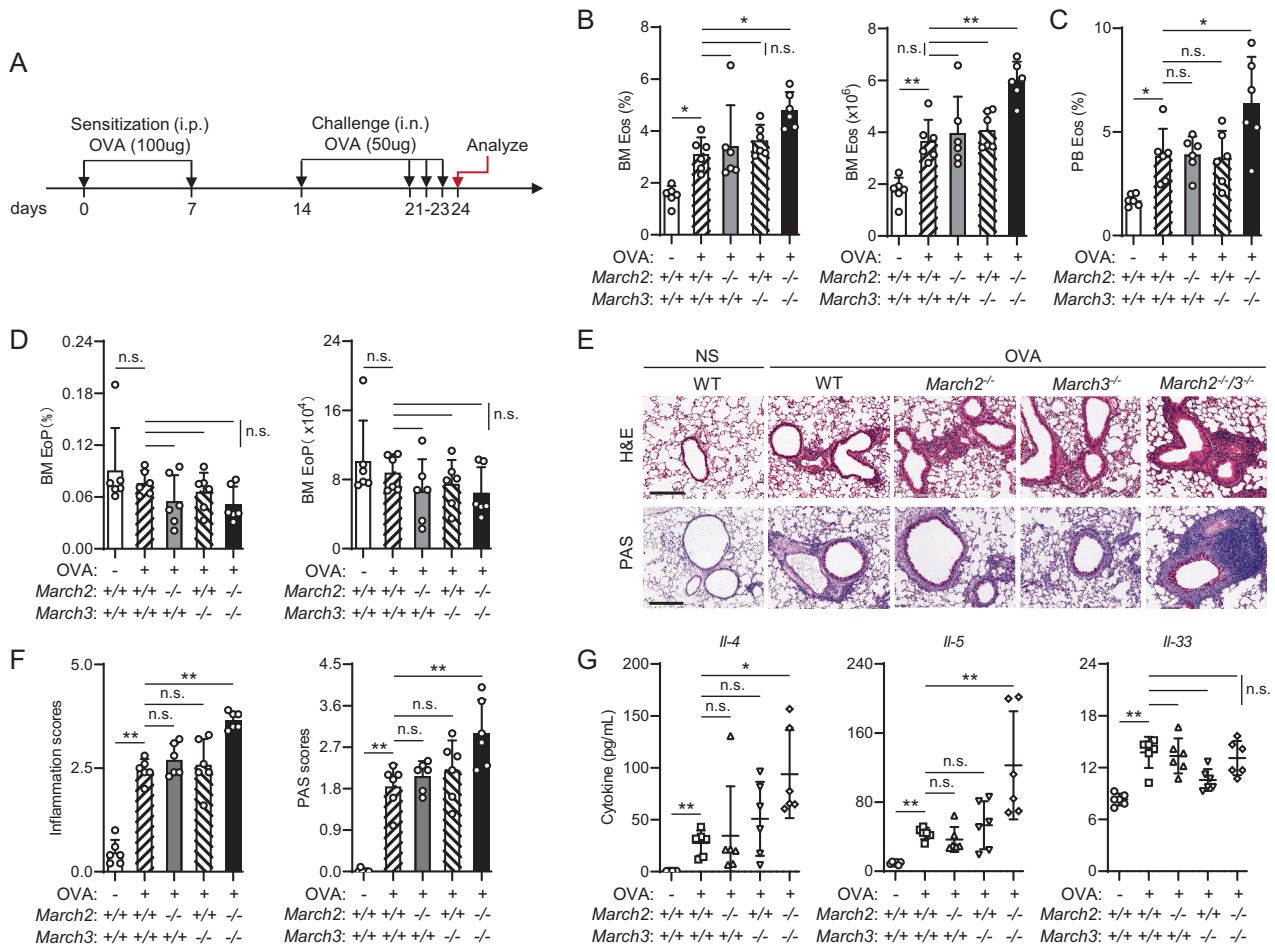


Fig. 5 March2/3 deficiency promotes eosinophilic airway inflammation. **A** A schematic timeline of the mouse model of allergic asthma. **B** Effects of March deficiency on the percentages and numbers of CCR3⁺Siglec-F⁺ eosinophils in the bone marrow. Bone marrow cells from OVA-challenged, age-matched wild-type, *March2*^{-/-}, *March3*^{-/-} and *March2*^{-/-}/*3*^{-/-} mice were collected 24 h after the final OVA challenge and analyzed by flow cytometry. The data shown are the means \pm SDs; $n = 6$ mice per group. **C** Effects of March deficiency on the percentage of CCR3⁺Siglec-F⁺ eosinophils in the peripheral blood. Peripheral blood leukocytes from OVA-challenged, age-matched wild-type, *March2*^{-/-}, *March3*^{-/-} and *March2*^{-/-}/*3*^{-/-} mice were collected 24 h after the final OVA challenge and analyzed by flow cytometry. The data shown are the means \pm SDs; $n = 6$ mice per group. **D** Effects of March deficiency on the percentages and numbers of Lin⁺CD34⁺Sca1^{c-}Kit^{int}II-5ra⁺ eosinophil progenitors in the bone marrow. Bone marrow cells from OVA-challenged, age-matched wild-type, *March2*^{-/-}, *March3*^{-/-} and *March2*^{-/-}/*3*^{-/-} mice were collected 24 h after the final OVA challenge and analyzed by flow cytometry. The data shown are the means \pm SDs; $n = 6$ mice per group. **E** H&E and PAS staining of lung tissues. OVA-challenged, age-matched wild-type, *March2*^{-/-}, *March3*^{-/-} and *March2*^{-/-}/*3*^{-/-} mice were sacrificed 24 h after the final OVA challenge. Lung tissues were collected, fixed with 4% paraformaldehyde and embedded in paraffin. The sections were stained with hematoxylin and eosin (H&E) or periodic acid-Schiff (PAS). Scale bar, 200 μ m. **F** Histological inflammation scores. Immune cell infiltration and peribronchial mucus production were scored based on the above H&E- and PAS-stained sections. The data shown are the means \pm SDs; $n = 6$ mice per group, 4–5 images per mouse. **G** Effects of March deficiency on the levels of IL-4, IL-5 and IL-33 in the peripheral blood. Sera from OVA-challenged, age-matched wild-type, *March2*^{-/-}, *March3*^{-/-} and *March2*^{-/-}/*3*^{-/-} mice were collected 24 h after the final OVA challenge for ELISA. The data shown are the means \pm SDs; $n = 6$ mice per group. WT wild-type. * $P < 0.05$; ** $P < 0.01$; n.s. not significant. The data in (B)–(G) were combined from two independent experiments

eosinophils [32]. To investigate whether March2/3 play roles in OVA-induced allergic airway inflammation, we evaluated the mRNA levels of March2 and March3 in lungs under steady-state conditions and during allergic airway inflammation. The results indicated that the transcription of March2 and March3 was slightly upregulated in the lungs under allergic conditions, suggesting that March2 and March3 might be involved in the negative feedback regulation of allergic airway inflammation (Fig. S3A). The proportions and numbers of mature eosinophils in the bone marrow following OVA challenges were significantly increased in *March2*^{-/-}/*3*^{-/-} mice in comparison to wild-type mice, whereas they were comparable between wild-type and *March2*^{-/-} or *March3*^{-/-} mice (Fig. 5B). These results suggest that March2/3 negatively regulates eosinophil lineage differentiation in the bone marrow during airway inflammation in a redundant manner.

Consistent with this finding, OVA-challenged *March2*^{-/-}/*3*^{-/-} mice had a larger percentage of eosinophils in the peripheral blood than that in wild-type mice (Fig. 5C). We further investigated the accumulation of eosinophils in the lungs, and the results indicated that the proportions and numbers of eosinophils were increased in the lungs of March2/3 DKO mice following OVA challenge (Fig. S3B). In contrast, the proportions and numbers of EoPs in the bone marrow were not markedly changed in *March2*^{-/-}/*3*^{-/-} mice (Fig. 5D). Hematoxylin-eosin (HE) staining showed that OVA-challenged wild-type mice exhibited inflammatory cell peribronchial and perivascular infiltration, and March2/3 deficiency dramatically enhanced inflammatory infiltration (Fig. 5E, F). Periodic acid-Schiff (PAS) staining showed that OVA-challenged *March2*^{-/-}/*3*^{-/-} mice displayed more bronchial mucus production than did wild-type mice (Fig. 5E, F). In addition, the levels of typical

Th2 cytokines, including Il-4 and Il-5, in the peripheral blood of *March2^{-/-}/3^{-/-}* mice following OVA challenge were increased in comparison to those in wild-type, *March2^{-/-}* and *March3^{-/-}* mice (Fig. 5G). In these experiments, the level of Il-33 was not affected by deficiency of *March2* or *March3* alone or in combination (Fig. 5G). Then, we explored whether *March2* or *March3* deficiency affects the production of type 2 cytokines by CD4⁺ T cells. The results indicated that *March2/3* double deficiency had no marked effect on the production of Il-4 and Il-5 in Th2 cells (Fig. S3C).

We further investigated whether the effects of *March2/3* double knockout on eosinophilic airway inflammation are mediated by increased Il-5 signaling activity. We sensitized mice and then pretreated them with an anti-Il-5 neutralizing antibody or control IgG following OVA challenge (Fig. 6A). OVA-induced eosinophilia in the bone marrow and lungs was attenuated following pretreatment with the anti-Il-5 antibody in both wild-type and *March2^{-/-}/3^{-/-}* mice, and the enhanced effects of *March2/3* double deficiency were suppressed (Fig. 6B, C). However, the proportion of lung Th2 cells was not markedly changed in *March2^{-/-}/3^{-/-}* mice in either the anti-Il-5 antibody or control IgG group (Fig. 6D), indicating that *March2* or *March3* deficiency has no marked effect on the OVA challenge-induced Th2 response. HE and PAS staining showed that the OVA-induced inflammatory cell infiltration and mucus production in lungs were reduced following pretreatment with the anti-Il-5 antibody both in wild-type and *March2^{-/-}/3^{-/-}* mice and that the enhanced effects of *March2/3* double deficiency were alleviated (Fig. 6E, F). Consistent with this finding, the level of the Th2 cytokine Il-4 was comparable between wild-type and *March2^{-/-}/3^{-/-}* mice when pretreated with the anti-Il-5 antibody (Fig. 6G). These results suggest that *March2* and *March3* play redundant roles in the negative regulation of eosinophil-driven allergic airway inflammation and hyperresponsiveness by targeting Il-5 signaling.

Deficiency of *March2/3* in hematopoietic cells is responsible for eosinophilic airway inflammation

To exclude a nonhematopoietic role of *March2/3* in airway inflammation, five groups of reciprocal bone marrow chimeric mice were generated by adoptive transfer of bone marrow into lethally irradiated recipients. Eight weeks after bone marrow transplantation and reconstitution, these bone marrow chimeric mice were subjected to OVA challenge (Fig. 7A). The results showed that wild-type and *March2/3*-deficient mice transplanted with hematopoietic cells from *March2/3*-deficient mice (DKO > WT and DKO > DKO, respectively) were more susceptible to OVA-induced airway inflammation than wild-type and *March2/3*-deficient mice transplanted with hematopoietic cells from wild-type mice (WT > WT and WT > DKO, respectively), as determined by the increased number of eosinophils in the bone marrow (Fig. 7B) and peripheral blood (Fig. 7C), enhanced peribronchial and perivascular inflammatory cell infiltration (Fig. 7D, E), increased bronchial mucus production (Fig. 7D, E) and increased levels of the Th2 cytokine Il-4 (Fig. 7F). In addition, WT > WT mice developed airway inflammation as severe as that in WT > DKO mice, as did DKO > WT mice and DKO > DKO mice (Fig. 7B–F). Collectively, these results indicate that *March2/3*-deficient hematopoietic cells are responsible for the aggravation of OVA-induced eosinophilic airway inflammation.

DISCUSSION

Interleukin 5 (IL-5) plays a crucial role in type 2-high asthma by mediating eosinophil maturation, activation, chemotaxis and survival [2, 30]. Most previous studies on the regulation of IL-5 signaling have focused on its downstream signaling events, and where and how it is regulated at the receptor level are largely unknown. In this study, we identified the plasma membrane-associated E3 ubiquitin ligases MARCH2 and MARCH3 as important negative regulators of

IL-5-triggered signaling by targeting IL-5R α for K27-linked polyubiquitination and lysosomal degradation. Our studies also demonstrated that MARCH2/3 function redundantly to negatively regulate eosinophil maturation and eosinophil-driven allergic airway inflammation and hyperresponsiveness.

Our results suggest that MARCH2 and MARCH3 negatively regulate IL-5-triggered signaling by mediating K27-linked polyubiquitination and lysosomal degradation of IL-5R α . Overexpression of MARCH2 or MARCH3 promoted the degradation of IL-5R α , which was inhibited by the lysosomal inhibitor NH₄Cl, whereas MARCH2 or MARCH3 deficiency had the opposite effects. These results suggest that MARCH2/3 mediates lysosomal degradation of IL-5R α . Coimmunoprecipitation experiments indicated that MARCH2 and MARCH3 constitutively interacted with IL-5R α . After IL-5 stimulation, the association between MARCH2 and IL-5R α was slightly enhanced, while the association between MARCH3 and IL-5R α was slightly decreased. In addition, MARCH2 or MARCH3 deficiency increased the IL-5R α level in both unstimulated and IL-5-stimulated cells. These results suggest that MARCH2/3 function constitutively in mediating IL-5R α downregulation.

MARCH2 and MARCH3 are members of the MARCH E3 ubiquitin ligase family. Overexpression of MARCH2 or MARCH3 but not their inactive mutants mediated K27-linked ubiquitination and degradation of IL-5R α . Interestingly, our results indicated that MARCH2 targets K379 of IL-5R α for K27-linked polyubiquitination, whereas MARCH3 targets K383 of IL-5R α for K27-linked polyubiquitination. It is possible that the subtle structural difference between the two MARCH proteins causes them to preferentially target these two adjacent residues in IL-5R α . Mutation of these residues in IL-5R α rendered it resistant to MARCH2/3-mediated K27-linked polyubiquitination and degradation. Reconstitution experiments indicated that the mutant of IL-5R α in which both K379 and K383 are mutated to arginine was more effective in mediating the transcription of downstream effector genes. These results suggest that MARCH2 and MARCH3 target two adjacent residues in IL-5R α for K27-linked polyubiquitination and lysosomal degradation, therefore negatively regulating IL-5-triggered signaling.

Previous studies have demonstrated that MARCH family proteins are involved in the regulation of immune responses by targeting certain immune receptors. MARCH3 and MARCH8 negatively regulate IL-1 β -triggered signaling by mediating K48-linked polyubiquitination and lysosomal degradation of IL-1RI and IL-1RAcP, respectively [21, 22]. MARCH3 mediates K48-linked polyubiquitination and lysosomal degradation of the IL-6 receptor and gp130, thereby negatively regulating colitis-associated carcinogenesis [23]. In this study, our results suggest that MARCH2 and MARCH3 target IL-5R α for K27-linked polyubiquitination and lysosomal degradation. These studies indicate that different MARCH family members or the same MARCH protein can catalyze distinct linkage types of polyubiquitination, suggesting the versatile regulatory effects of MARCH proteins on distinct immune receptors.

The MARCH family contains 11 members, which have been categorized into four subgroups based on phylogenetic analysis. MARCH2 and MARCH3 are largely similar and classified into the same subgroup. Our studies suggest that MARCH2 and MARCH3 play redundant roles in the negative regulation of IL-5R α . Deficiency of either MARCH2 or MARCH3 only modestly increased the IL-5R α level, IL-5-induced phosphorylation of STAT5 and transcription of downstream effector genes, whereas double knockout of MARCH2/3 had more dramatic effects. This functional redundancy was also observed in mice. Flow cytometric analysis indicated that *March2^{-/-}/3^{-/-}* mice exhibited a significantly larger population of eosinophils in the bone marrow and peripheral blood, whereas *March2^{-/-}* or *March3^{-/-}* mice had no marked or only modest increases in these eosinophil populations in comparison to those in wild-type mice. In the OVA-induced asthma model, the mRNA levels of *March2* and *March3* were slightly increased in the lungs, suggesting that *March2* and

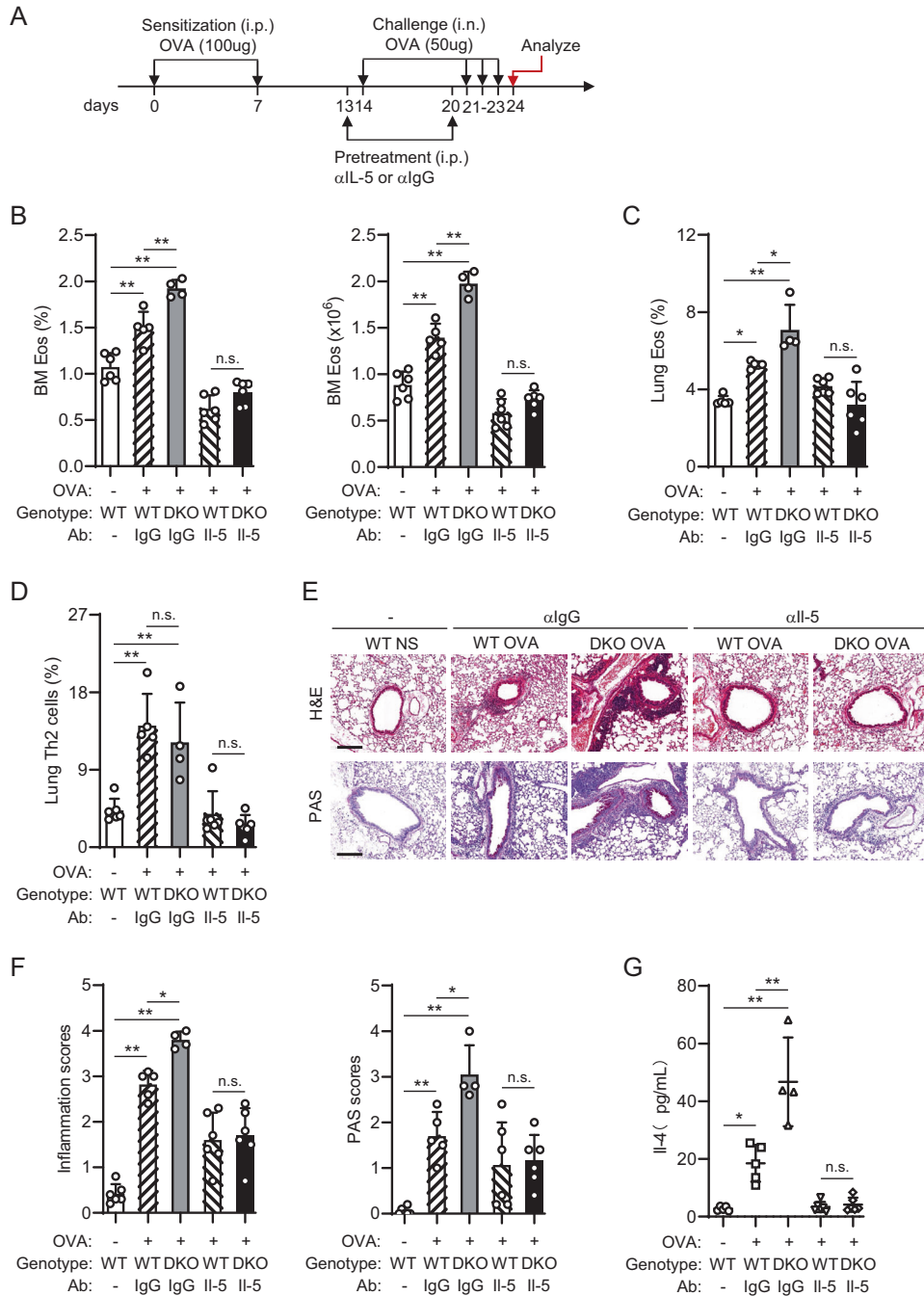


Fig. 6 *March2/3* regulates eosinophilic airway inflammation by targeting *Il-5* signaling. **A** schematic timeline of allergic asthma model establishment and neutralizing antibody pretreatment in mice. **B** Effects of neutralization of *Il-5* on the percentages and numbers of $CCR3^+Siglec-F^+$ eosinophils in the bone marrow. Bone marrow cells from the indicated pretreated and OVA-challenged age-matched wild-type and *March2^{-/-}/3^{-/-}* mice were collected 24 h after the final OVA challenge and analyzed by flow cytometry. The data shown are the means \pm SDs; $n = 4-6$ mice per group from one representative experiment. Effects of neutralization of *Il-5* on the percentages of $CCR3^+Siglec-F^+$ eosinophils (**C**) and $CD3^+CD4^+ST2^+$ Th2 cells (**D**) in lung tissues. Lung single-cell suspensions from the indicated pretreated and OVA-challenged age-matched wild-type and *March2^{-/-}/3^{-/-}* mice were collected 24 h after the final OVA challenge and analyzed by flow cytometry. The data shown are the means \pm SDs; $n = 4-6$ mice per group from one representative experiment. **E** H&E and PAS staining of lung tissues. The indicated pretreated and OVA-challenged age-matched wild-type and *March2^{-/-}/3^{-/-}* mice were sacrificed 24 h after the final OVA challenge. Lung tissues were collected, fixed with 4% paraformaldehyde and embedded in paraffin. The sections were stained with hematoxylin and eosin (H&E) or periodic acid-Schiff (PAS). Scale bar, 200 μ m. **F** Histological inflammation scores. Immune cell infiltration and peribronchial mucus production were scored based on the above H&E- and PAS-stained sections. The data shown are the means \pm SDs; $n = 4-6$ mice per group from one representative experiment, 4-5 images per mouse. **G** Effects of neutralization of *Il-5* on the level of *Il-4* in the peripheral blood. Sera from the indicated pretreated and OVA-challenged age-matched wild-type and *March2^{-/-}/3^{-/-}* mice were collected 24 h after the final OVA challenge for ELISA. The data shown are the means \pm SDs; $n = 4-6$ mice per group from one representative experiment. WT wild-type. * $P < 0.05$; ** $P < 0.01$; n.s. not significant

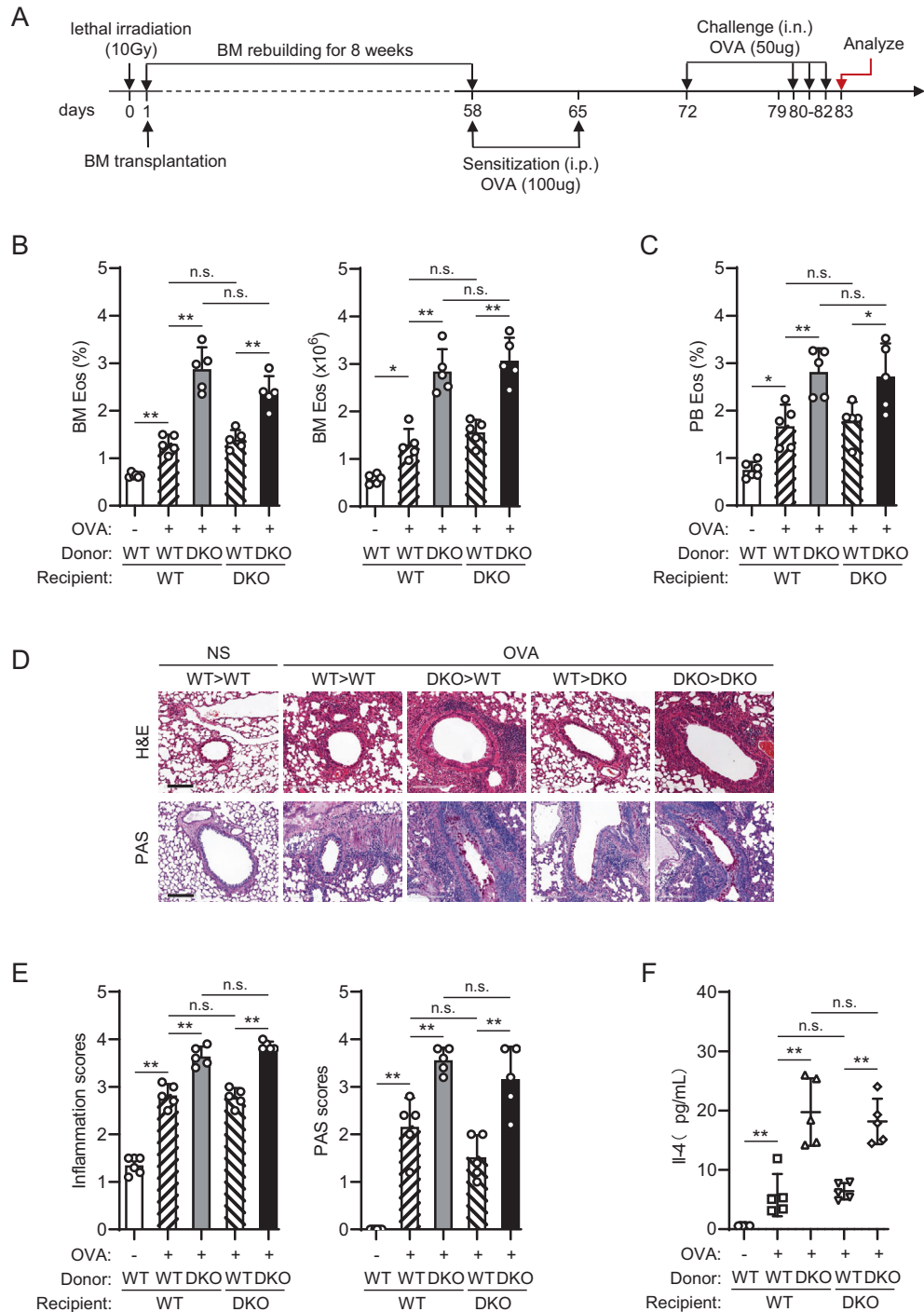


Fig. 7 Deficiency of MARCH2/3 in hematopoietic cells is responsible for eosinophilic airway inflammation. **A** A schematic timeline of mouse bone marrow transplantation and allergic asthma model establishment. **B** Effects of bone marrow transplantation on the percentage and number of CCR3⁺Siglec-F⁺ eosinophils in the bone marrow. Bone marrow cells from OVA-challenged, age-matched wild-type and *March2*^{-/-}/*3*^{-/-} bone marrow chimeric mice were collected 24 h after the final OVA challenge and analyzed by flow cytometry. The data shown are the means ± SDs; *n* = 5–6 mice per group from one representative experiment. **C** Effects of bone marrow transplantation on the percentage of CCR3⁺Siglec-F⁺ eosinophils in peripheral blood. Peripheral blood leukocytes from OVA-challenged, age-matched wild-type, and *March2*^{-/-}/*3*^{-/-} bone marrow chimeric mice were collected 24 h after the final OVA challenge and analyzed by flow cytometry. The data shown are the means ± SDs; *n* = 5–6 mice per group from one representative experiment. **D** H&E and PAS staining of lung tissues. OVA-challenged, age-matched wild-type and *March2*^{-/-}/*3*^{-/-} bone marrow chimeric mice were sacrificed 24 h after the final OVA challenge. Lung tissues were collected, fixed with 4% paraformaldehyde and embedded in paraffin. The sections were stained with hematoxylin and eosin (H&E) or periodic acid-Schiff (PAS). Scale bar, 200 μm. **E** Histological inflammation scores. Immune cell infiltration and peribronchial mucus production were scored based on the above H&E- and PAS-stained sections. The data shown are the means ± SDs; *n* = 5–6 mice per group from one representative experiment, 4–5 images per mouse. **F** Effects of bone marrow transplantation on the level of IL-4 in the peripheral blood. Sera from OVA-challenged, age-matched wild-type and *March2*^{-/-}/*3*^{-/-} bone marrow chimeric mice were collected 24 h after the final OVA challenge for ELISA. The data shown are the means ± SDs; *n* = 5–6 mice per group from one representative experiment. WT wild-type. **P* < 0.05; ***P* < 0.01; n.s. not significant

March3 might be involved in the negative feedback regulation of allergic airway inflammation. The proportions of mature eosinophils in the bone marrow, peripheral blood and lungs and the levels of typical Th2 cytokines, including IL-4 and IL-5, in the peripheral blood following OVA challenge were significantly increased in *March2*^{-/-}/*3*^{-/-} mice in comparison to wild-type mice, whereas they were comparable between wild-type mice and both *March2*^{-/-} and *March3*^{-/-} mice. Consistent with this finding, OVA-challenged *March2*^{-/-}/*3*^{-/-} mice had greater inflammatory infiltration and more bronchial mucus production than did wild-type mice. Pretreatment with the anti-IL-5 antibody attenuated OVA-induced inflammation in both wild-type and *March2*^{-/-}/*3*^{-/-} mice and suppressed the enhanced effects of March2/3 deficiency. March2/3-deficient hematopoietic cells are responsible for aggravation of OVA-induced eosinophilic airway inflammation. In conclusion, our findings indicate that MARCH2 and MARCH3 play redundant roles in the negative regulation of IL-5-triggered eosinophil maturation and eosinophilic airway inflammation by targeting IL-5Rα for K27-linked polyubiquitination and lysosomal degradation. Our study reveals a regulatory mechanism of IL-5-triggered effects at the receptor level, which may be considered for the development of therapeutic interventions for inflammatory airway diseases.

MATERIALS AND METHODS

Reagents and antibodies

The following items were purchased from the indicated companies: RNAiso Plus (Takara Bio, 9109); M-MLV reverse transcriptase (Invitrogen, 28025-013); RiboLock RNase Inhibitor (Thermo Scientific, EO0382); SYBR Green (Bio-Rad, 172-5274); MG132 (MCE, HY-13259); 3-MA (MCE, 5142-23-4); polybrene (Millipore, TR-1003-G); RPMI-1640 medium (Gibco, C11875500BT); Dulbecco's modified Eagle's medium (Gibco, C11995500BT); fetal bovine serum (FBS; CellMAX, SA211.02); penicillin/streptomycin (Gibco, 15140-122); ELISA kits for mouse IL-4 (BioLegend, 431101), IL-5 (BioLegend, 431204) and IL-33 (R&D Systems, DY3626-05); recombinant human IL-5, GM-CSF, and murine IL-5 (Peprotech, 200-05, 300-03 and 215-15, respectively); mouse monoclonal antibodies against IL-3/IL-5/GM-CSFRβ (Santa Cruz Biotechnology, sc-398246), FLAG[®] M2 (Sigma-Aldrich, F3165), β-actin (Sigma-Aldrich, A2228), hemagglutinin (HA; BioLegend, 901515), and Myc (Cell Signaling Technology, 2276); rabbit antibodies against p-Y694/699-STAT5 (Cell Signaling Technology, 4322), STAT5 (Cell Signaling Technology, 94205), human IL-5Rα (Abxexa, abx103030), murine March2 (Abcam, ab220292), and ubiquitin linkage-specific K27 (Abcam, ab181537); a goat antibody against human IL-5Rα (Thermo Fisher, PA5-47340); HRP-conjugated mouse anti-HA (Sigma Aldrich, H6533); monoclonal anti-FLAG[®] M2-HRP (Sigma-Aldrich, A8592); mouse anti-goat IgG-HRP (Santa Cruz Biotechnology, sc-2354); goat anti-rabbit IgG HRP (Abmart, M21007); anti-mouse Ig HRP (Rockland Immunochemicals, 18-8817-33); and anti-rabbit IgG HRP (Rockland Immunochemicals, 18-8816-33). Mouse antiserum against MARCH3 was raised against recombinant human MARCH3 (aa 10-180). Mouse antiserum against IL-5Rα was raised against recombinant human IL-5Rα (aa 21-420). Rabbit antiserum against MARCH2 was raised against recombinant human MARCH2 (aa 1-137).

Cells

HEK293 and TF-1 cells were obtained from ATCC. HEK293 cells were cultured in Dulbecco's modified Eagle's medium supplemented with 10% FBS and 1% penicillin-streptomycin. TF-1 cells [33] were cultured in RPMI-1640 medium supplemented with 10% FBS, 1% penicillin-streptomycin and 2 ng/mL GM-CSF.

Establishment of the IL-5-dependent TF-1 cell line

TF-1-IL5 cells stably expressing human IL-5Rα have been described previously [34]. TF-1 cells were cultured with recombinant IL-5 (2 ng/mL) but not GM-CSF for one month. The surviving cells were subcloned and expanded to establish the IL-5-dependent cell line, which was designated TF-1-IL-5.

Constructs

Mammalian expression plasmids for the following proteins were constructed by standard molecular biology techniques: FLAG-, HA- or

Myc-tagged MARCH1-11 and the corresponding mutants; IL-5Rα and its mutants; IL-5Rβ; JAK1; JAK2; STAT5A; STAT5B; and Ub and its mutants. Plasmids expressing guide RNAs (gRNAs) targeting MARCH2, MARCH3 and IL5Rα were constructed with the lentiCRISPR V2 vector.

Mice

March2^{-/-} and *March3*^{-/-} mice were generated as previously described [23]. *March2*^{-/-}/*3*^{-/-} mice were obtained by breeding *March2*^{-/-} mice with *March3*^{-/-} mice. Mice were maintained in a special pathogen-free facility at the Medical Research Institute at Wuhan University. All mouse studies were approved by the Animal Care Committee of the Medical Research Institute of Wuhan University.

Transfection

HEK293 cells were transfected by standard calcium phosphate precipitation. An empty control plasmid was added to ensure that each transfectant received the same amount of total DNA.

Retroviral-mediated gene transfer

HEK293 cells plated in 100-mm dishes were transfected with pMSCV-PuroR (10 μg) together with the pGag-Pol (10 μg) and pVSV-G (3 μg) plasmids. Two days after transfection, viruses were harvested for infection of TF-1-IL5 cells in the presence of polybrene (8 μg/mL) for 24 h. Infected cells were selected with puromycin (2 μg/mL) for at least 7 days.

CRISPR/Cas9 gene editing

The CRISPR/Cas9 system was previously described [24, 25]. In brief, double-stranded oligonucleotides corresponding to the target sequences were inserted into the lentiCRISPR V2 plasmid, which was transfected with the packaging plasmid psPAX2 and the envelope plasmid pMD2.G into HEK293 cells. Two days after transfection, viruses were harvested for infection of TF-1-IL5 cells in the presence of polybrene (8 μg/mL). One day later, infected cells were selected with puromycin (2 μg/mL) for at least 7 days. The following oligonucleotides were used to construct the corresponding gRNA plasmids.

gNC: 5'-GTAGTCGGTACGTGACTCGT-3';
 gIL-5Rα: 5'-GTAGTGAGTGGTCTGTTCTGC-3';
 gMARCH2 #1: 5'-GCCCGTAGCTCCACGACTC-3';
 gMARCH2 #2: 5'-CCACATACTGGGGCGGTCCG-3';
 gMARCH3 #1: 5'-TGCACCCGTGGTGAAGACGG-3';
 gMARCH3 #2: 5'-GATTGTGGCAGCCTAGTGAA-3'.

Coimmunoprecipitation, ubiquitination assay and immunoblot analysis

Cells were lysed in 1 mL of pre-lysis buffer (20 mM Tris-HCl, 150 mM NaCl, 1 mM EDTA, 1% Triton X-100, 10 μg/mL aprotinin, 10 μg/mL leupeptin, and 1 mM phenylmethylsulfonyl fluoride). For each immunoprecipitation reaction, a 0.4 mL aliquot of lysate was incubated with 1 μg of the indicated antibody or control IgG and 35 μL of a 1:1 slurry of Protein G Sepharose (GE Healthcare) at 4 °C for 3 h. The Sepharose beads were washed three times with 1 mL of lysis buffer containing 500 mM NaCl. The precipitates were separated by sodium dodecyl sulfate-polyacrylamide gel electrophoresis (SDS-PAGE), and immunoblot analysis was performed with the indicated antibodies.

For ubiquitination assays, the immunoprecipitates were re-extracted in pre-lysis buffer containing 1% SDS and denatured by heating for 10 min. The supernatants were diluted with regular lysis buffer until the concentration of SDS was decreased to 0.1% and were reimmunoprecipitated with the indicated antibodies. These immunoprecipitates were analyzed by immunoblotting with the anti-ubiquitin antibody. For endogenous coimmunoprecipitation and immunoblotting experiments, the indicated cells were starved overnight in medium with 0.5% FBS and stimulated with IL-5 and GM-CSF for the indicated times or left untreated before coimmunoprecipitation and immunoblot analysis.

qPCR

Total RNA was isolated from cells using TRIzol reagent, reverse transcribed and subjected to qPCR analysis to measure the mRNA levels of the tested genes. The data shown are the relative abundances of the indicated mRNAs normalized to the abundance of human *GAPDH* or mouse *Gapdh*. qPCR was performed using the following primers.

Human *GAPDH*: GTCTCTGACTTCAACAGCG (forward) and ACCACCCTGTTGCTGAGCCAA (reverse);

Human *ID1*: GTTGAGCTGAACTCGGAATCC (forward) and ACACAAGA TGCGATCGTCCGCA (reverse);
 Human *PIM1*: TCTACTAGGCATCCGCTCTC (forward) and CTTCAGCAG GACCACTTCCATG (reverse);
 Human *CD69*: GCTGGACTTACGCCAAAATGC (forward) and AGTCCA ACCCAGTGTTCCTCTC (reverse);
 Human *FOS*: GCCTCTTACTACCACTCACC (forward) and AGATGGCAGT GACCGTGGGAAT (reverse);
 Human *IL-5Ra*: TGACTGGCTTGCGGTGCTTGT (forward) and CTGCTG TGACATTCAGTGGAGG (reverse);
 Mouse *Gapdh*: CATCACTGCCACCCAGAAGACTG (forward) and ATGCCA GTGAGCTTCCCGTTTCAG (reverse);
 Mouse *Id1*: TTGTCTGTCCGAGCAAAGCGT (forward) and CGTGAGTAGC AGCCGTTTCATG (reverse);
 Mouse *Cish*: GGATCTGTGTCATAGCCAAG (forward) and CTCGAAGTAC GAATGTACCTCC (reverse);
 Mouse *Socs3*: GGACCAAGAACCTACGCATCCA (forward) and CACCAGCT GAGTACACAGTCG (reverse).

Confocal microscopy

HEK293 cells were transfected with the indicated plasmids by standard calcium phosphate precipitation. Twenty hours after transfection, the cells were treated with 200 nM LysoTracker Red DND-99 (Thermo Fisher, L7528) for 1 h, fixed with 4% paraformaldehyde for 15–20 min and then washed with phosphate-buffered saline (PBS) 3 times. Images were acquired using a Zeiss LSM880 confocal microscope with a 63x oil objective.

Flow cytometry and cell sorting

To analyze the cellular composition in the peripheral blood (100 μ L/mouse) and spleen, tissues were collected from WT, *March2^{-/-}*, *March3^{-/-}* and *March2^{-/-}/3^{-/-}* mice for preparation of single-cell suspensions. After depletion of red blood cells, the remaining cells were stained with the following antibodies: anti-CD11b-Percp Cyanine5.5 (eBioscience, 45-0112-82), anti-CD11b-APC (BD Biosciences, 553312), anti-CCR3-FITC (R&D, FAB729F), anti-SiglecF-PE (BD Biosciences, 552126), anti-CD4-PE (BD Biosciences, 553048), anti-CD8-Pacific Blue (BD Biosciences, 558106), anti-CD3-FITC (BD Biosciences, 561801) and anti-B220-APC (BD Biosciences, 553092).

For analysis of eosinophils and progenitors in the bone marrow, both the femurs and tibias from individual mice were collected and flushed with cold PBS. After depletion of red blood cells, single-cell suspensions were prepared using a 100 μ m cell strainer (BD Falcon). Cells were counted with a TC20 automated cell counter (Bio-Rad), and 1×10^6 cells were taken for analysis. For eosinophils, cells were stained with anti-CD11b-Percp Cyanine5.5 (eBioscience, 45-0112-82), anti-CCR3-FITC (R&D, FAB729F), anti-SiglecF-PE (BD Biosciences, 552126), and anti-CD125-PE Cyanine7 (BioLegend, 153408) antibodies. For analysis of progenitors, cells were first stained with a cocktail of biotin-conjugated anti-mouse lineage of antibodies, including antibodies against Ter-119, Gr-1 (Ly6G/Ly6C), CD11b, CD45R/B220 and CD3e (all from BioLegend, 133307), to label lineage-negative (Lin⁻) cells and then stained with the following antibodies: Streptavidin-PE (BioLegend, 410504), anti-c-Kit-APC eFluor 780 (eBioscience, 47-1172-82), anti-Sca-1-Pacific Blue (BioLegend, 122519), anti-CD34-APC (BioLegend, 119309), anti-CD16/32-PE Cyanine7 (eBioscience, 25-0161-81), anti-CD16/32 (clone 93, BD Biosciences) and anti-CD125/IL-5Ra-Alexa Fluor 488 (BD Biosciences, 558533). For eosinophil isolation, bone marrow single-cell suspensions were collected and stained with anti-CCR3-FITC (R&D, FAB729F) and anti-SiglecF-PE (BD Biosciences, 552126) antibodies.

Peritoneal cell suspensions were harvested in cold PBS. Red blood cells were lysed with hypotonic ACK solution. After lysis of red cells, the cell suspensions were washed with PBS, and the cell density was adjusted to 10^6 cells/mL. Peritoneal cells were then stained with anti-B220-APC (BD Biosciences, 553092), IgM-FITC (BD Biosciences, 553408), anti-CD19-PE (BD Biosciences, 557399) and anti-CD125-PE Cyanine7 (BioLegend, 153408) antibodies.

For analysis of eosinophils and Th2 cells in lung tissues, lung lobes were cut into small segments and were then minced and digested in calcium- and magnesium-free HBSS containing 10 μ g/ml type II collagenase (Worthington) and 20 μ g/ml DNase I (Sigma-Aldrich, 18068-015) for 1 h at 37 °C. Digested lung tissues were gently ground and filtered to obtain single-cell suspensions. Cells were stained with the following antibodies: anti-CD11b-Percp Cyanine5.5 (eBioscience, 45-0112-82), anti-CCR3-FITC (R&D, FAB729F), anti-SiglecF-PE (BD Biosciences, 552126), anti-CD125-PE Cyanine7 (BioLegend, 153408), anti-CD4-PE (BD Biosciences, 553048), anti-CD4-FITC (BD Biosciences, 553046), anti-CD3-FITC (BD Biosciences, 561801),

anti-ST2-APC (eBioscience, 17-9335-82), anti-IL-4-PerCP-eFluor 710 (eBioscience, 46-7041-82) and anti-IL-5-eFluor 450 (eBioscience, 48-7052-82). All staining was performed at 4 °C for 30 min in the dark. The gating strategies are described in the related figure legends. BD LSRFortessaX-20 and FACSCelesta instruments were used for cell analysis, and a BD FACSARIA III instrument was used for cell sorting at the Flow Cytometry Core Facility of the Medical Research Institute. Data were analyzed using FlowJo™ 10 software.

OVA-induced airway inflammation and pretreatment with a neutralizing antibody in mice

The OVA sensitization and challenge procedures were modified from a published study [35]. Six- to eight-week-old mice were used to establish the asthma models. In brief, on Days 0 and 7, mice were sensitized by a single intraperitoneal injection of 100 μ g of OVA (Sigma-Aldrich) diluted with 100 μ L of normal saline (NS) and then mixed with 4 mg of Imject™ Alum (100 μ L per animal, Thermo Scientific, 77161) in a total volume of 200 μ L. On Days 14 and 21–23, experimental mice were anesthetized with 1% phenobarbital sodium by intraperitoneal injection and challenged intranasally with 20 μ L of normal saline containing 50 μ g of OVA. Control mice were sensitized with an equal volume of normal saline and Imject™ Alum mixture and challenged intranasally with an equal volume of normal saline at each time point. To neutralize the bioactivity of IL-5, mice were pretreated with 1 mg/kg anti-IL-5 mAb (BioLegend, 504315, TRFK5) or control rat IgG (BioLegend, 400457) in 500 μ L of normal saline by intraperitoneal injection on Days 13 and 20. Control mice were pretreated i.p. with an equal volume of normal saline at each time point. Mice were killed 24 h after the last challenge for data analysis.

Bone marrow chimeras

To exclude the contribution of nonhematopoietic roles of March2/3 in airway inflammation, bone marrow chimeric mice were generated as previously described [36].

In brief, 7-week-old recipient mice were sublethally irradiated (10 Gy) and intravenously injected with 1×10^7 bone marrow cells isolated from 7- to 8-week-old wild-type or March2/3-deficient mice 24 h after irradiation. Bone marrow reconstitution was performed reciprocally, resulting in the generation of four groups of experimental mice. The recipient mice were housed for 8 weeks for full reconstitution of the bone marrow before being treated with OVA.

Histology

Lungs were collected from mice 24 h after the last OVA challenge and fixed by immersion in 4% paraformaldehyde. Lung lobes were sectioned, embedded in paraffin, sliced into 5 μ m sections and stained with hematoxylin and eosin (H&E) for analysis of inflammatory cell infiltrates or with periodic acid-Schiff (PAS) for analysis of mucus production. The scores of peribronchiolar and perivascular inflammation were determined as previously described [37]. The degree of airway inflammation was scored on a scale of 0 to 4, with 0 indicating negative PAS staining and 1 to 4 indicating positive PAS staining in bronchi. The extent of mucus production in PAS-positive bronchi was scored as follows: 1, 5–25%; 2, 25–50%; 3, 50–75%; and 4, 75% of cells with positive PAS staining. Peribronchiolar and perivascular inflammation was scored as follows: 0, normal; 1, few inflammatory cells; 2, a ring of inflammatory cells one cell layer deep; 3, a ring of inflammatory cells two to four cells deep; and 4, a ring of inflammatory cells more than four cells deep.

Statistical analysis

For comparisons between two groups, data were analyzed by an unpaired *t* test. When more than two groups were compared, data were analyzed by one-way or two-way ANOVA. All statistical analyses were performed with GraphPad Prism 8, and differences with a *P* value < 0.05 were considered statistically significant.

DATA AVAILABILITY

All data needed to evaluate the conclusions in the paper are presented in the paper. The materials described in the study are either commercially available or available upon request from the corresponding author.

REFERENCES

- Yanagibashi T, Satoh M, Nagai Y, Koike M, Takatsu K. Allergic diseases: From bench to clinic - contribution of the discovery of interleukin-5. *Cytokine*. 2017;98:59–70.
- Dougan M, Dranoff G, Dougan SK. GM-CSF, IL-3, and IL-5 family of cytokines: regulators of inflammation. *Immunity*. 2019;50:796–811.
- Wu D, Molofsky AB, Liang HE, Ricardo-Gonzalez RR, Jouihan HA, Bando JK, et al. Eosinophils sustain adipose alternatively activated macrophages associated with glucose homeostasis. *Science*. 2011;332:243–7.
- Hammad H, Lambrecht BN. The basic immunology of asthma. *Cell*. 2021;184:1469–85.
- FitzGerald JM, Bleecker ER, Nair P, Korn S, Ohta K, Lommatzsch M, et al. Benralizumab, an anti-interleukin-5 receptor alpha monoclonal antibody, as add-on treatment for patients with severe, uncontrolled, eosinophilic asthma (CALIMA): a randomised, double-blind, placebo-controlled phase 3 trial. *Lancet*. 2016;388:2128–41.
- Rothenberg ME. Humanized anti-IL-5 antibody therapy. *Cell*. 2016;165:509.
- Castro M, Zangrilli J, Wechsler ME, Bateman ED, Brusselle GG, Bardin P, et al. Reslizumab for inadequately controlled asthma with elevated blood eosinophil counts: results from two multicentre, parallel, double-blind, randomised, placebo-controlled, phase 3 trials. *Lancet Respir Med*. 2015;3:355–66.
- Pavord ID, Korn S, Howarth P, Bleecker ER, Buhl R, Keene ON, et al. Mepolizumab for severe eosinophilic asthma (DREAM): a multicentre, double-blind, placebo-controlled trial. *Lancet*. 2012;380:651–9.
- Tomaki M, Zhao LL, Lundahl J, Sjostrand M, Jordana M, Linden A, et al. Eosinophilopoiesis in a murine model of allergic airway eosinophilia: involvement of bone marrow IL-5 and IL-5 receptor alpha. *J Immunol*. 2000;165:4040–50.
- Broughton SE, Dhagat U, Hercus TR, Nero TL, Grimbaldeston MA, Bonder CS, et al. The GM-CSF/IL-3/IL-5 cytokine receptor family: from ligand recognition to initiation of signaling. *Immunol Rev*. 2012;250:277–302.
- Ogata N, Kouro T, Yamada A, Koike M, Hanai N, Ishikawa T, et al. JAK2 and JAK1 constitutively associate with an interleukin-5 (IL-5) receptor alpha and beta subunit, respectively, and are activated upon IL-5 stimulation. *Blood*. 1998;91:2264–71.
- Takaki S, Kanazawa H, Shiiba M, Takatsu K. A critical cytoplasmic domain of the interleukin-5 (IL-5) receptor alpha chain and its function in IL-5-mediated growth signal transduction. *Mol Cell Biol*. 1994;14:7404–13.
- Stout BA, Bates ME, Liu LY, Farrington NN, Bertics PJ. IL-5 and granulocyte-macrophage colony-stimulating factor activate STAT3 and STAT5 and promote Pim-1 and cyclin D3 protein expression in human eosinophils. *J Immunol*. 2004;173:6409–17.
- Yun Y, Kanda A, Kobayashi Y, Van Bui D, Suzuki K, Sawada S, et al. Increased CD69 expression on activated eosinophils in eosinophilic chronic rhinosinusitis correlates with clinical findings. *Allergol Int*. 2020;69:232–8.
- Sonkin D, Palmer M, Rong X, Horrigan K, Regnier CH, Fanton C, et al. The identification and characterization of a STAT5 gene signature in hematologic malignancies. *Cancer Biomark*. 2015;15:79–87.
- Kagami S, Nakajima H, Kumano K, Suzuki K, Suto A, Imada K, et al. Both stat5a and stat5b are required for antigen-induced eosinophil and T-cell recruitment into the tissue. *Blood*. 2000;95:1370–7.
- Zhu Y, Chen L, Huang Z, Alkan S, Bunting KD, Wen R, et al. Cutting edge: IL-5 primes Th2 cytokine-producing capacity in eosinophils through a STAT5-dependent mechanism. *J Immunol*. 2004;173:2918–22.
- Samji T, Hong S, Means RE. The Membrane Associated RING-CH Proteins: A Family of E3 Ligases with Diverse Roles through the Cell. *Int Sch Res Not*. 2014;2014:637295.
- Lin H, Li S, Shu HB. The Membrane-Associated MARCH E3 Ligase Family: Emerging Roles in Immune Regulation. *Front Immunol*. 2019;10:1751.
- Zheng C. The emerging roles of the MARCH ligases in antiviral innate immunity. *Int J Biol Macromol*. 2021;171:423–7.
- Chen R, Li M, Zhang Y, Zhou Q, Shu HB. The E3 ubiquitin ligase MARCH8 negatively regulates IL-1beta-induced NF-kappaB activation by targeting the IL1RAP coreceptor for ubiquitination and degradation. *Proc Natl Acad Sci USA* 2012;109:14128–33.
- Lin H, Gao D, Hu MM, Zhang M, Wu XX, Feng L, et al. MARCH3 attenuates IL-1beta-triggered inflammation by mediating K48-linked polyubiquitination and degradation of IL-1RI. *Proc Natl Acad Sci USA* 2018;115:12483–8.
- Lin H, Feng L, Cui KS, Zeng LW, Gao D, Zhang LX, et al. The membrane-associated E3 ubiquitin ligase MARCH3 downregulates the IL-6 receptor and suppresses colitis-associated carcinogenesis. *Cell Mol Immunol*. 2021;18:2648–59.
- Sanjana NE, Shalem O, Zhang F. Improved vectors and genome-wide libraries for CRISPR screening. *Nat Methods*. 2014;11:783–4.
- Shalem O, Sanjana NE, Hartenian E, Shi X, Scott DA, Mikkelsen T, et al. Genome-scale CRISPR-Cas9 knockout screening in human cells. *Science*. 2014;343:84–7.
- Nakamura N. The role of the transmembrane RING finger proteins in cellular and organelle function. *Membr (Basel)*. 2011;1:354–93.
- Chathuranga K, Kim TH, Lee H, Park JS, Kim JH, Chathuranga WAG, et al. Negative regulation of NEMO signaling by the ubiquitin E3 ligase MARCH2. *EMBO J*. 2020;39:e105139.
- Akashi K, Traver D, Miyamoto T, Weissman IL. A clonogenic common myeloid progenitor that gives rise to all myeloid lineages. *Nature*. 2000;404:193–7.
- Iwasaki H, Mizuno S, Mayfield R, Shigematsu H, Arinobu Y, Seed B, et al. Identification of eosinophil lineage-committed progenitors in the murine bone marrow. *J Exp Med*. 2005;201:1891–7.
- Rothenberg ME, Hogan SP. The eosinophil. *Annu Rev Immunol*. 2006;24:147–74.
- Brusselle GG, Maes T, Bracke KR. Eosinophils in the spotlight: Eosinophilic airway inflammation in nonallergic asthma. *Nat Med*. 2013;19:977–9.
- Lambrecht BN, Hammad H, Fahy JV. The Cytokines of Asthma. *Immunity*. 2019;50:975–91.
- Kitamura T, Tange T, Terasawa T, Chiba S, Kuwaki T, Miyagawa K, et al. Establishment and characterization of a unique human cell line that proliferates dependently on GM-CSF, IL-3, or erythropoietin. *J Cell Physiol*. 1989;140:323–34.
- Fu Z, Yu C, Wang L, Gao K, Xu G, Wang W, et al. Development of a robust reporter gene based assay for the bioactivity determination of IL-5-targeted therapeutic antibodies. *J Pharm Biomed Anal*. 2018;148:280–7.
- Casaro M, Souza VR, Oliveira FA, Ferreira CM. OVA-induced allergic airway inflammation mouse model. *Methods Mol Biol*. 2019;1916:297–301.
- Zhang HX, Xu ZS, Lin H, Li M, Xia T, Cui K, et al. TRIM27 mediates STAT3 activation at retromer-positive structures to promote colitis and colitis-associated carcinogenesis. *Nat Commun*. 2018;9:3441.
- Tong J, Bandulwala HS, Clay BS, Anders RA, Shilling RA, Balachandran DD, et al. Fas-positive T cells regulate the resolution of airway inflammation in a murine model of asthma. *J Exp Med*. 2006;203:1173–84.

ACKNOWLEDGEMENTS

We thank Deng Gao, Xuemei Yi, Mi Li, Ru Zang, Chen Li, and Li Zhong for technical help and academic discussions and sincerely appreciate all the staff at the core facility of the Medical Research Institute at Wuhan University for their technical support. This work was supported by grants from the National Natural Science Foundation of China (32188101, 31830024 and 32070775), the CAMS Innovation Fund for Medical Sciences (2019-I2M-5-071) and the Fundamental Research Funds for the Central Universities.

AUTHOR CONTRIBUTIONS

SL, H-BS, and L-WZ conceived and designed the study. L-WZ, LF, RL, and HL performed the experiments. SL, L-WZ, and H-BS analyzed the data and wrote the manuscript.

COMPETING INTERESTS

The authors declare no competing interests.

ADDITIONAL INFORMATION

Supplementary information The online version contains supplementary material available at <https://doi.org/10.1038/s41423-022-00907-9>.

Correspondence and requests for materials should be addressed to Shu Li.

Reprints and permission information is available at <http://www.nature.com/reprints>

Springer Nature or its licensor holds exclusive rights to this article under a publishing agreement with the author(s) or other rightsholder(s); author self-archiving of the accepted manuscript version of this article is solely governed by the terms of such publishing agreement and applicable law.